International Journal of Pharmaceutics 397 (2010) 36–43

Contents lists available at ScienceDirect

International Journal of Pharmaceutics

journal homepage: www.elsevier.com/locate/ijpharm

Parallel stacking of caffeine with riboflavin in aqueous solutions: The potential mechanism for hydrotropic solubilization of riboflavin

Yong Cui*

Small Molecule Pharmaceutical Sciences, Genentech, Inc., 1 DNA Way, South San Francisco, CA 94080, United States

ARTICLE INFO

Article history:
Received 25 April 2010
Received in revised form 6 June 2010
Accepted 22 June 2010
Available online 30 June 2010

Keywords:
Molecular dynamics simulation
Hydrotropy
Solubilization
Complexation
Parallel stacking

ABSTRACT

Hydrotropy is a phenomenon where the presence of a large quantity of one solute enhances the solubility of another solute. The mechanism of this phenomenon remains elusive and a topic of debate. This study employed molecular dynamics simulation to investigate solute interactions of a model system consisting of a hydrotropic agent, caffeine (CAF), a poorly water-soluble solute, riboflavin (RBF), and water. The study demonstrates that CAF and RBF undergo molecular parallel stacking in the aqueous solution, a result correlating closely to the self-stacking of CAF under the same conditions. The correlations are found both structurally and dynamically, suggesting that the self-stacking of CAF is the primary effect, and incorporation of RBF is the secondary effect. The solute stacking gives rise to the partitioning of solutes and water, which helps restoring the normal water structure and drives down the system energy. The interactions between the solutes are found insignificant to the solute clustering. The dynamic data confirm that the solute stacks are dynamically active. These results suggest that hydrotropic effect of CAF may be attributed to solute parallel stacking.

1. Introduction

Hydrotropic solubilization is an important technique in promoting drug aqueous solubility (Boylan, 1986). Numerous studies have been devoted to elucidate the nature and mechanisms of this phenomenon (Coffman and Kildsig, 1996a; Rasool et al., 1991; Cheema et al., 2007; Oberoi et al., 2005), which led to proposals of several potential mechanisms, including complexation, "salting-in", changes in the nature of the solvent (Coffman and Kildsig, 1996b), and molecular aggregation (Agrawal et al., 2004). Nevertheless, contradictory observations are often reported, as summarized briefly in a recent communication (Cui et al., 2010). One example is the debate concerning with the role of aromaticity vs. hydrophobicity in hydrotropic solubilization. Neuberg (1916) was the first to note that the aromatic ring was crucial to the hydrotropic effect. This observation was later rationalized by molecular orbital calculations, which suggested that the aromatic ring or ring system may facilitate a π-donor π-acceptor interaction (Fawzi et al., 1980; Hata et al., 1967). Rasool et al. (1991) also showed that aromatic ring systems may promote stacking of molecules, and, as a result, enhanced drug aqueous solubility more effectively than the aliphatic amides (e.g., urea and its derivatives). Nevertheless, experimental findings inconsistent to this potential mechanism were also reported. For example, NA was shown to solubilize drugs in the absence of a π-donor π-acceptor interaction (Coffman and Kildsig, 1996a). It was also found that the hydrophobicity, rather than the aromaticity, of hydrotropic agents is the determinant of their solubilization ability (Kenley et al., 1986; Suzuki and Sunada, 1980). These seemingly contradictory observations have so far not been resolved successfully.

The complexity of elucidating hydrotrcopic mechanisms arises partially from the apparent drug-hydrotrope selectivity and the structural diversity of hydrotropic agents (HAs) (Lee et al., 2003; Shah and Flanagan, 1990). While the former suggests that the mechanisms of hydrotropy could be system-specific, the latter boosts up the difficulty and workload of addressing the issue. It is often the case where a potential mechanism apparently plausible to one hydrotropic system may be inapplicable to another. To achieve adequate structure-specific understanding of the hydrotropic effect, it is necessary to examine a diverse collection of hydrotropic systems with techniques of molecular-level resolutions.

In light of this situation, we initiated a series of studies using molecular dynamics (MD) simulation to probe hydrotropic solubilization. In an earlier study (Cui et al., 2010), we successfully modeled the solubilization effect of nicotinamide, a commonly used hydrotropic agents. The results clearly show that the solubilization is driven by non-stoichiometric molecular aggregation. The π-donor π-acceptor interaction and the so-induced molecular stacking, on the other hand, are not apparent. It is somewhat unexpected that molecular stacking was not found for nicotinamide in aqueous solution since it is a flat heteroaromatic compound. This

* Tel.: +1 650 467 1402; fax: +1 650 225 3613.
E-mail address: ycui@gene.com.

0378-5173/$ – see front matter © 2010 Elsevier B.V. All rights reserved.
doi:10.1016/j.ijpharm.2010.06.043

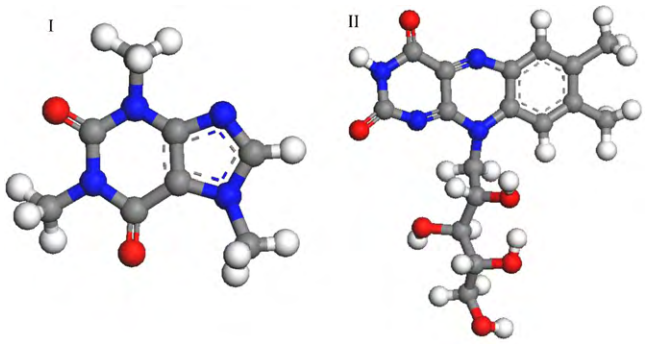

Fig. 1. Molecular configurations of caffeine (I) and riboflavin (II).

brings up a question: would all hydrotropic solubilizations arise from the non-stoichiometric molecular aggregation as demonstrated by the nicotinamide system, or would the molecular stacking also play a role? To address this question, we extend the study to caffeine, another heteroaromatic HA whose solubilization mechanism has been believed with some certainty to be the parallel stacking of the solutes (Coffman and Kildsig, 1996a).

Caffeine (CAF) and nicotinamide (NA) share many important structural features. In addition to being heteroaromatic compounds, both agents present planer molecular configurations, and both were found self-aggregate in aqueous solutions (Birdsall et al., 1973; Falk et al., 1990). Furthermore, a previous study employing NMR spectrometry suggested that both CAF and NA formed complexes via molecular stacking with riboflavin (Evstigneev et al., 2005; Veselkov et al., 2002). Thus, the hydrotropic solubilization mechanisms are often considered the same for these two agents (Evstigneev et al., 2006). Moreover, additional studies on hydrotropic solubilization of CAF favored that CAF formed complexes via molecular stacking with other aromatic drugs (Davies et al., 2001a,b). These results give rise to a discrepancy: if CAF develops molecular parallel stacking as suggested by the reports above and NA undergoes a non-stoichiometric molecular aggregation as indicated in our previous simulation study (Cui et al., 2010), they shall then take different modes of clustering in aqueous solutions. Otherwise, either our previous report on NA system or these reports could be inaccurate. Therefore, studying CAF system is of particular interests both to clarify the hydrotropic mechanism of CAF and to attest the reliability of the simulation approach employed in our studies.

The study employed model systems consisting of riboflavin (RBF), a poorly-soluble B-class vitamin, solubilized by CAF in an aqueous environment (see Fig. 1 for chemical structures of RBF and CAF). Hydrotropic solubilization of RBF was previously reported in the presence of CAF (Guttman and Athalye, 1960). In the current study we focused on the interactions between RBF and CAF molecules in aqueous solutions, and attempted to deduce the hydrotropic mechanism from the interactions. Evidence directly related to the solubilization effect, i.e., the free energy change, was not readily accessible through our MD simulations. Notwithstanding this disadvantage, the knowledge acquired on solute interactions still supplies rich insights to the potential solubilization mechanism. Furthermore, the self-aggregation of CAF in aqueous solutions was also investigated in this study.

2. Computational method

The solubility of RBF (MW 376.4) in 0.1 M CAF aqueous solution (pH 7) is 1.27 mM, an approximately 3.3-fold enhancement relative to that in water (Guttman and Athalye, 1960). This translates to an approximate molar ratio of RBF:CAF:H_2O = 0.069:6:3000. Granted this experimental result, a model system was constructed consisting of one RFB and six CAF randomly dispersed in 3000 water molecules (RBF + CAF + Water system) as our primary model. Both RBF and CAF were treated unionized in the model.

The model was set up using the Amorphous Cell module of the Material Studio 4.3 software package. A cubic simulation box with periodic boundary conditions in all directions was constructed with a density of 1 g/cm^3 and a side length of about 45 Å. Two solutes, RBF and CAF, were randomly dispersed in water molecules by a modified Markov process, followed by geometric optimization of molecular configurations utilizing COMPASS force field. COMPASS is a Class II *ab initio* force field designed for use with organic molecules and optimized for the simulation of condensed phases (Hwang et al., 1994; Sun, 1998; Bunte and Sun, 2000). Fig. 1 shows the optimized molecular configurations of RBF and CAF. Both molecules have almost flat planary configurations. The MD simulation was carried out under NPT conditions in the Forcite module of MS, with pressure and temperature held at 100 kPa and 298 K, respectively, by employing Nose thermostat and Berendsen barostat. The COMPASS force field was used to calculate both van der Waals and electrostatic interactions. Charge groups were applied with cut-off distances of 15.5 Å for both interactions. The time step was 1 fs and the simulation time was at least 2.5 ns.

To study self-aggregation of CAF in the aqueous solution in the absence of RBF, another simulation box was built in the same manner but consisted of only six CAF and 3000 water molecules (CAF + Water system), followed by a MD run performed under the same conditions as above. Furthermore, to assist the analysis of both energetic and dynamic changes upon hydrotropic solubilization, a couple of additional systems were prepared and subsequently subjected to the NPT runs using the same method as above. The details are provided in the next section.

Data analysis was performed using the Forcite Analysis function. In calculating radial distribution functions, molecular centroids of RBF and CAF were used. The oxygen atom was selected for water as it was the only heavy atom in the water molecule. The calculation cut-off distance and step size were set at 35 and 0.1 Å, respectively. For mean square displacements, molecular centroids were chosen, and the calculation was conducted in the last 1 ns of simulations with a step size of 1 ps and a calculation length of 500 ps. In hydrogen bonding (HB) calculation, a cut-off distance of 2.5 Å was applied and the HBs were averaged over the first and last 10 frames (10 ps) with a step size of 1 ps.

3. Results and discussion

The initial states of both RBF + CAF + Water and CAF + Water systems were homogeneous solutions, as shown in Fig. 2A and C. After simulations, parallel stacking of RBF and CAF molecules, or stacking of CAF molecules themselves, was observed for the RBF + CAF + Water and the CAF + Water systems, respectively, as evidenced by Fig. 2B and D. The RBF molecule was sandwiched in the stack of CAF molecules, as shown in the magnified image in Fig. 3. The hydrophilic ribose group of RBF, as expected, protruded into the water medium. One CAF molecule lied on top of the stack, another CAF molecule had been floating in the media. The progression of the stacking process can be seen in Fig. 4. In the case of the RBF + CAF + Water system, two smaller stacks formed by 0.5 ns, with one consisting of RBF and two CAF molecules, and the other of two CAFs (Fig. 4A). These two stacks moved closer at 1 ns, with one consisting of four molecules (Fig. 4B). By 1.5 ns the RBF and five CAFs stacked in parallel to each other, with the last CAF floating in the media (Fig. 4C). This lasted for 2 ns until the floating CAF clustered with the stack at 3.5 ns (Fig. 4D). However, this cluster appeared not stable, and the last CAF molecule drifted away again by 4 ns (Fig. 4E).

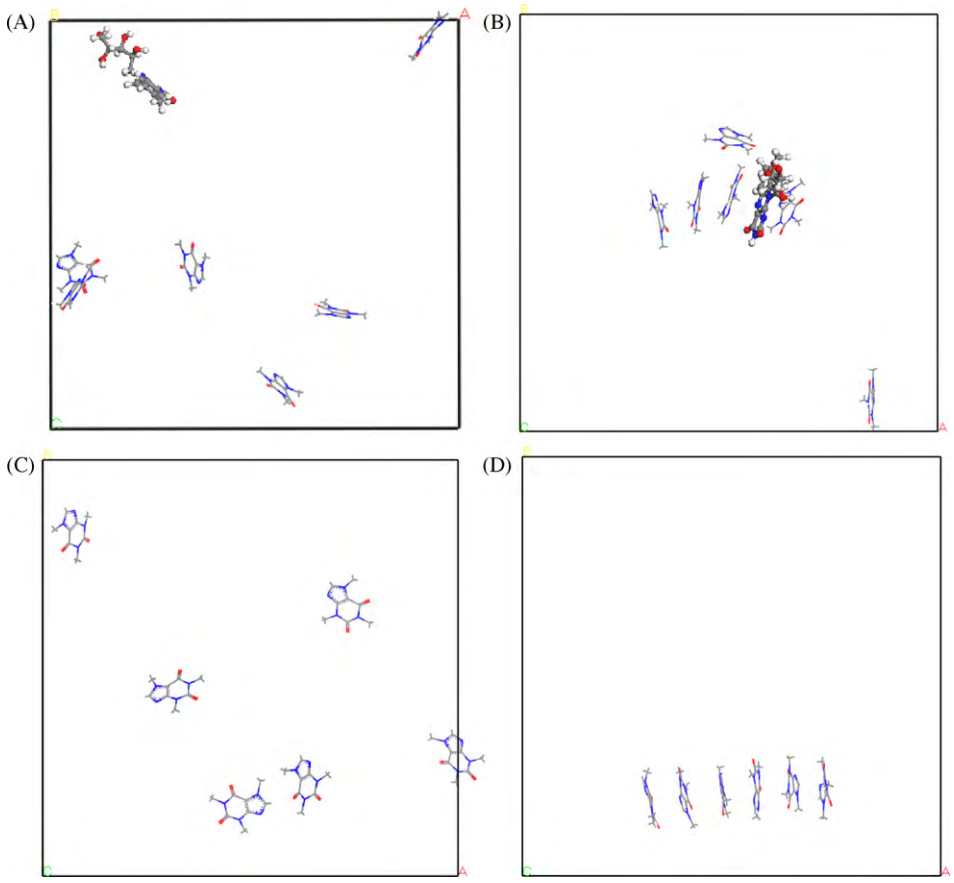

Fig. 2. Snapshots of MD simulations of one riboflavin (ball and stick) and six caffeine (line) in 3000 water molecules system (RBF + CAF + Water system) as well as six caffeine in 3000 water molecules system (CAF + Water system). Water molecules are deleted for the sake of clarity. (A) RBF + CAF + Water system, $t = 0$ ns; (B) RBF + CAF + Water system, $t = 6$ ns; (C): CAF + Water system, $t = 0$ ns; (D) RBF + CAF + Water system, $t = 4$ ns.

Meanwhile, the dynamic movement of the stack was also evident, and the stack was not always in a perfect straight line (Fig. 4E). Finally, the stack stabilized by 5 ns (Fig. 4F) and lasted to the end of the run (6 ns). Throughout the simulation the last CAF molecule maintained a floating state except in a brief period between 3.2 and 3.6 ns. Given this observation and the prolonged simulation time (6 ns), it seems that the system has arrived the equilibrium state, where the last CAF can be stably floating in the system. The system energy, pressure, and cell parameters were also examined,

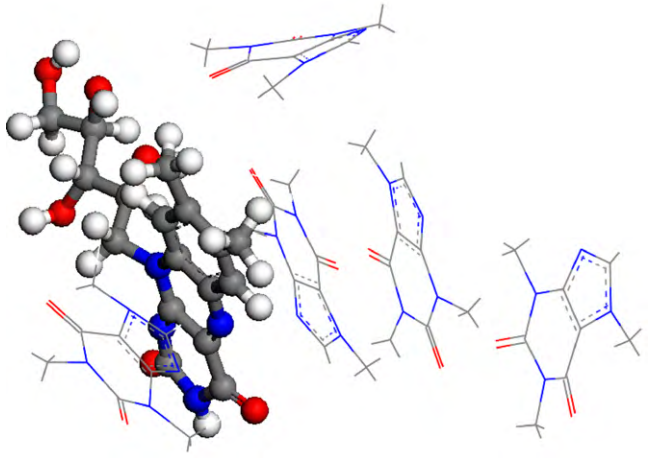

Fig. 3. Configurations of molecular stacking in the RBF + CAF + Water system after 6 ns. RBF in ball and stick and CAF in line.

and the results indicated the equilibrium state after 1.5 ns. We thus speculate that the floating CAF molecule may represent the solute concentration in the free (vs. the clustered) state. It is reasonable to believe that the clustered and the free solutes are in a dynamic equilibrium, where a portion of the solute is in the free state. If the result above is this case, it could imply that at the current concentration the system has reached the equilibrium, and further growth of the cluster size may not result in additional energy reduction. In other words, the cluster could have a size limit, where it may find equilibrium with the free portion of CAF in the solution. Although the actual size limit may be comparable to the one showed in this study, further simulations are required on larger systems at the same concentration to confirm this is the case. This effort was not pursued in the current work due to the limited computation power (the current system size is close to the limit of our computation capacity). Overall, this observation is slightly different from our study on the NA system (Cui et al., 2010), and additional discussions will be provided later in the text.

In the CAF + Water system, on the other hand, the equilibration seemed to take longer. Two smaller molecular stacks were observed by 2 ns (Fig. 5A). By 2.5 ns all six CAF molecules were clustered together, but still in two stacks perpendicular to each other (Fig. 5B). The completion of stacking process took another 1.5 ns. At 3 ns there is still one CAF not in parallel stack (Fig. 5C). This CAF further moved to one end of the stack, and induced the end CAF into a two-molecular stack in perpendicular to the rest CAFs (Fig. 5D). The final stack stabilized by 4 ns and lasted to the end of the run (5 ns). No apparent shifting in system energy, density, and temperature were seen after 3 ns. Overall, the results show that parallel stacking indeed occurs among CAF molecules as well as between

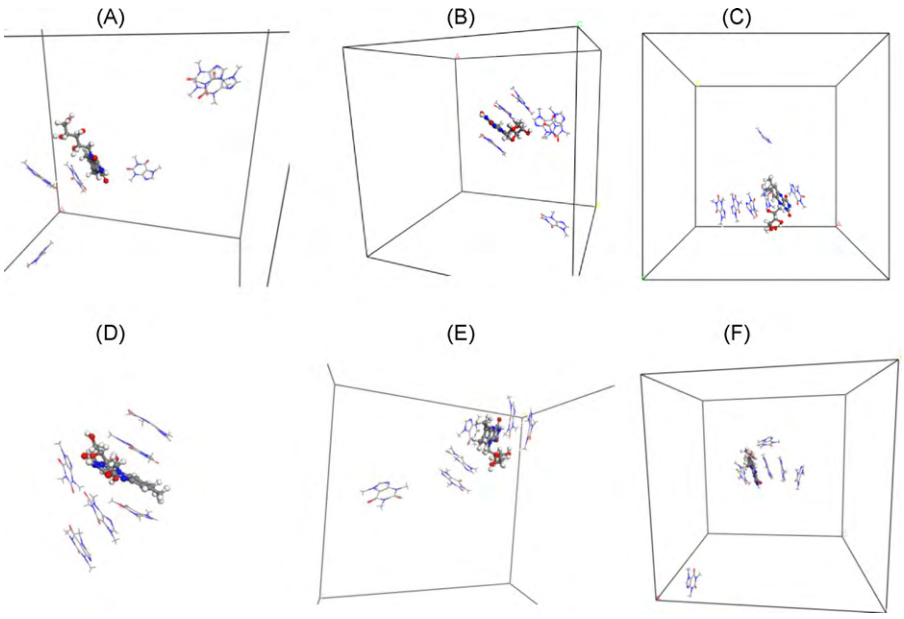

Fig. 4. Molecular clustering trajectory in the RBF + CAF + Water system (one riboflavin and six caffeines in 3000 water molecules). Riboflavin is in ball and stick, caffeine is in line. Water molecules are deleted for the sake of clarity. A: 0.5 ns; B: 1 ns; C: 1.5 ns; D: 3.5 ns; E: 4 ns; F: 5 ns.

the CAF and RBF, which is consistent to other reports on CAF solutions discussed in Section 1. Thus, it suggests that the mechanism of hydrotropic solubilization of CAF is different from that of NA.

The radial distribution functions (RDFs) provide a clear picture for the structural evolvement during the simulations. Fig. 6 depicts the averaged RDFs during the first 100 and the last 1000 ps within and between each type of molecules in the RBF + CAF + Water system. It is evident from Fig. 6A and B that RBF and CAF, as well as CAF molecules themselves, clustered together from a homogeneous solution state, in consistent to the visual observation from the snapshots. Meanwhile, a reduction in water concentration in the vicinity of RBF aroused from the clustering, as demonstrated in Fig. 6C, indicating that the stacking of RBF with CAF molecules reduced the exposure of the hydrophobic RBF to the surrounding water. In the case of CAF, a similar drop of water concentration in the neighborhood of CAF is also witnessed in Fig. 6D. Both results suggest that shunning away from water may be instrumental to the energy reduction of the system, and therefore could be critical in driving the parallel stacking of the CAF and the solute molecules.

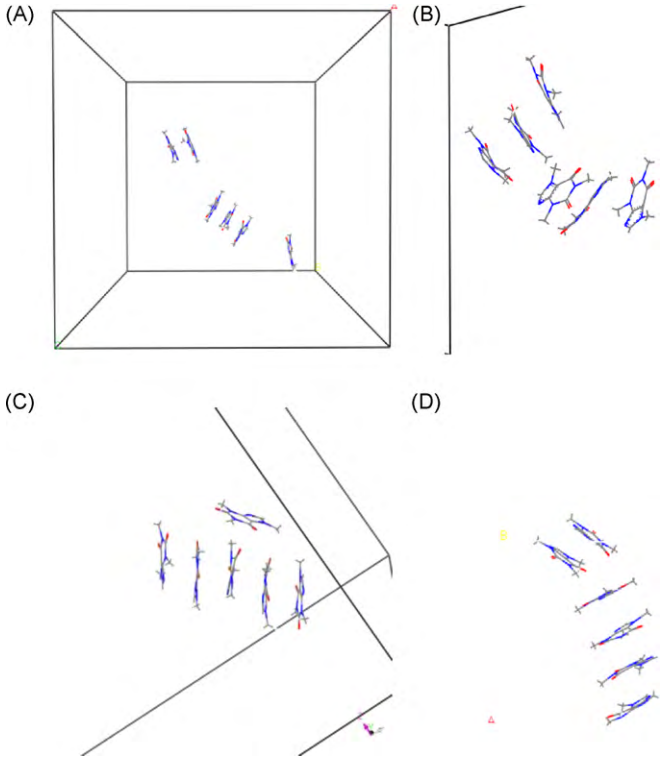

Fig. 5. Molecular clustering trajectory in the CAF + Water system (six caffeines in 3000 water molecules). Caffeine is in line. Water molecules are deleted for the sake of clarity. (A) 2 ns; (B) 2.5 ns; (C) 3 ns; and (D) 3.5 ns.

The RDFs of the CAF + Water system are given in Fig. 7. Panels (A and B) show the RDFs between CAF–CAF and CAF–Water molecules, respectively. The CAF–water RDF resembled closely to that of the RBF + CAF + Water system (Fig. 6D), while the CAF-CAF RDF presented qualitative similarity to, but differed significantly in the peak height from, that of the RBF + CAF + Water system (Fig. 6B). For the latter the calculation procedure was double-checked and no errors were found. The reason for this difference seems to be that in the CAF + Water system all six CAF molecules clustered together, while the cluster in the RBF + CAF + Water system only contained five CAF molecules. Since the averaged concentration of CAF in the whole system space was quite low due to the large box size and just a handful of CAFs, this minor difference actually produced a quite significant difference in the peak height in the RDFs. Irrespective of this difference, the results are in support of the conclusions drawn for the RBF + CAF + Water system that a reduction of water concentration in the neighborhood of CAF arises from the parallel stacking of CAF molecules. Finally, the water–water RDFs in both the RBF + CAF + Water and the CAF + Water systems were examined (data not shown), and no significant changes were observed upon simulations. To ensure that water structures in these models represented the bulk liquid water, an additional system was built containing 3000 water molecules (the Water system) only, followed by a 2.5 ns NPT run under the same conditions as described above. The water–water RDF of the Water system in the last 1 ns of the run (data not shown) was found overlapping with the ones from the RBF + CAF + Water and the CAF + Water systems, certifying that waters in these systems represented the bulk liquid water.

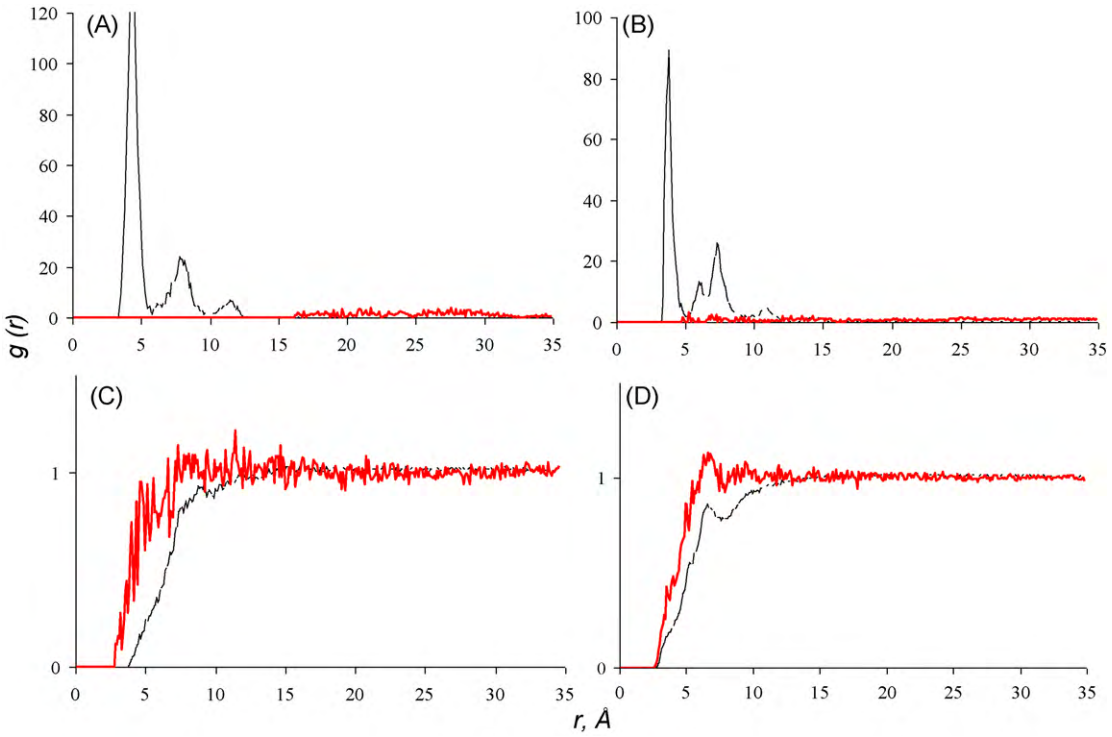

Fig. 6. Radial distribution functions of one riboflavin and six caffeine in 3000 water molecules (RBF + CAF + Water system). Black: 5–6 ns; red: 0–100 ps. (A) RBF–CAF; (B) CAF–CAF; (C) RBF–water; (D) CAF–water. (For interpretation of the references to color in this Fig. 6, the reader is referred to the web version of the article.)

To confirm that shunning away from water for the RBF and CAF molecules is instrumental to the energy reduction of the system, we further analyzed the changes in hydrogen bonds and system energies before and after simulations. Table 1 lists various types of HBs in the RBF + CAF + Water and the CAF + Water systems. It is evident that both systems were dominated by the water–water HBs (>99.4% of the total HBs) before and after simulations, dwarfing other types of HBs. Furthermore, upon simulations the water–water HBs registered significant gains, while the CAF–water and the RBF–water HBs both showed slight decreases. The CAF–RBF HBs, on the other hand, gave minor increases. These results are reasonable and consistent to the observed clustering of RBF and CAF molecules, which essentially partitioned the solutes from the solvent so that the HBs within the solvent and solutes were enhanced, respectively, while the HBs across the solvent and solutes were demoted. In a sense this is an exchange of solute–water HBs with that of the solute–solute and water–water HBs. The result of this exchange, however, is significant net gains in the total HBs in both systems, thanks obviously to the contribution from the enhanced water–water HBs. Meanwhile, the average HB bond length also presented declines in both systems (Table 1), indicating that the HB interactions on average turned stronger and therefore energetically more favorable owing to the parallel stacking of the solutes. A couple of observations are worth further noting: (1) a high correlation between the RBF + CAF + Water and the CAF + Water systems were found in terms of their HB changes upon simulations, suggesting that the self-stacking of CAF molecules is likely the foundation of the phenomenon, while incorporating RBF is just a side effect building on this effect. During the simulation the HBs between RBF and CAFs increased from one to three, almost trivial relative to the changes in water–water HBs, indicating that HB interactions between these two types of molecules are not the key driving force for the clustering. The fact that RBF undergoes parallel stacking with CAFs suggests that this process is likely to share the same mechanism with the self-stacking of CAF molecules; (2) it is interesting to note that no CAF-CAF HBs were established in both systems after the simulations, which clearly precludes the potential contribution to the self-stacking from the specific HB interactions among the CAF molecules. This shows that the primary driving force for parallel stacking, at least among CAF molecules, is the restoration of normal water structure as demonstrated by the recovery of water–water HBs in the systems. If, as discussed in (1), the parallel stacking of RBF with CAFs share the same mechanism with the self-stacking of CAF molecules, it is reasonable to project that the restoration of normal water structure is also the key driving force here; (3) the HBs in the Water system (containing 3000 water molecules only) after 2.5 ns run were also calculated and listed in Table 1. In comparison to the Water system, it is evident that the solutes in the homogeneous dispersion state indeed suppressed the HB interactions in both solution systems, and after solute clustering

Table 1
Hydrogen bonds in the RBF + CAF + Water and CAF + Water systems.

	t, ns	H_2O–H_2O	CAF–H_2O	RFN–H_2O	CAF–RFN	CAF–CAF	Total number of H-bonds ± SD	Average length of H-bonds ± SD, Å
RFN + CAF + Water	0	5589 ± 97	21 ± 2	12 ± 1	1 ± 1	0	5622 ± 97	1.9875 ± 0.0164
	6	5804 ± 43	17 ± 2	9 ± 1	3 ± 1	0	5832 ± 43	1.9683 ± 0.0033
CAF + Water	0	5597 ± 82	22 ± 3	–	–	0	5619 ± 82	1.9874 ± 0.0162
	5	5796 ± 31	16 ± 2	–	–	0	5812 ± 32	1.9685 ± 0.0026
Water	2.5						5808 ± 26	1.9676 ± 0.0022

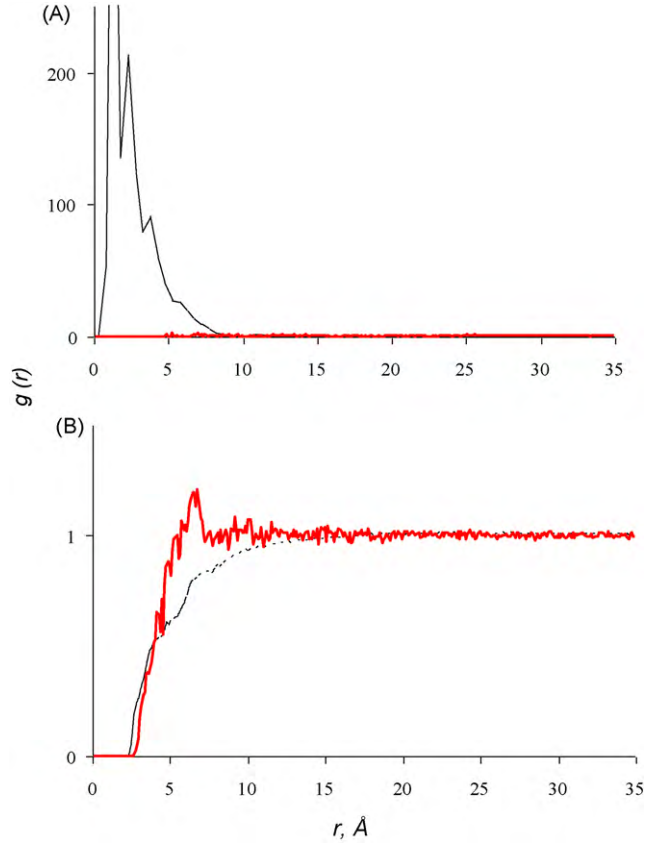

Fig. 7. Radial distribution functions of six caffeine in 3000 water molecules (CAF + Water system). Black: 3–4 ns; red: 0–100 ps. (A) CAF–CAF and (B) CAF–water. (For interpretation of the references to color in this figure legend, the reader is referred to the web version of the article.)

the system HBs almost recovered to the level of pure water system. This again supports that the restoration of water–water HBs occurred upon clustering. Meanwhile, the average bond length of water–water HBs in the pure Water system is the lowest, indicating that water–water HBs are energetically more favorable than other types of HBs in the systems.

The system energy changes upon equilibration are plotted in Fig. 8. Similar to the HB changes discussed above, various types of energy changes showed high correlation between the RBF + CAF + Water and the CAF + Water systems. The total energies presented, as expected, significant net gains upon equilibration, indicating that the parallel stacking of solutes are energetically favorable. Among various energy components, valence and van der Waals energies registered increases, which were offset by declines in electrostatic and HB energies. Evidently, the contribution of elec-

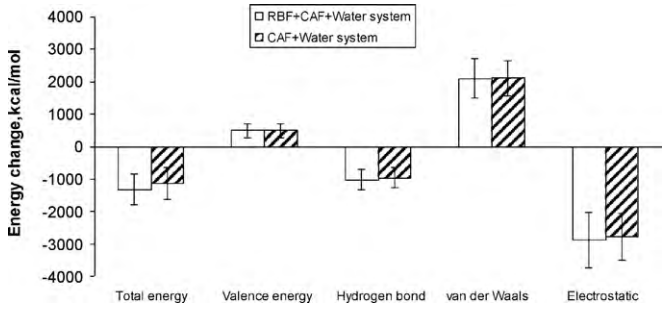

Fig. 8. Energy changes upon equilibration in the RBF + CAF + Water and CAF + Water systems.

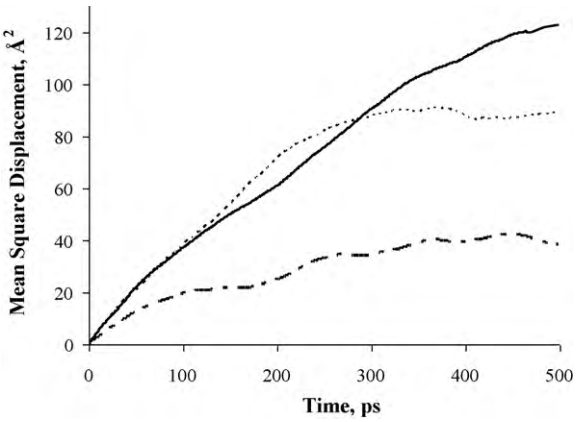

Fig. 9. Mean square displacements of centers of riboflavin and caffeine in three systems. Solid line: CAF molecules in the RBF + CAF + Water system; bold solid line: CAF molecules in the CAF + Water system; bold broken line: RBF molecule in the RBF + CAF + Water system; broken line: RBF molecule in the RBF + Water system.

trostatic energy is the most significant force driving the clustering of solutes. The HBs, on the other hand, accounted for approximately 78 84% of the net total energy gains in the RBF + CAF + Water and the CAF + Water systems, respectively, defining their significant role in the clustering process. Obviously, a majority of the contribution from the HBs aroused from water–water HBs rather than solute–solute interactions, as shown in the HB changes presented above. Combining these with the similar results reported in an other hydrotropic system (Cui et al., 2010), one conclusion seems to be in order: despite that molecular clustering, including molecular aggregation and parallel stacking, indeed demands some selective molecular properties of the solutes, it is likely more critical that these properties, upon solute clustering, give rise to water–water HB interactions than promote the specific solute–solute interactions. Thus, attentions paid towards the specific solute–solute interactions in hydrotropic systems, as many previous studies indicated, might need to be re-evaluated. On the other hand, solute–solute interactions may be critical in driving the solute clusters towards parallel stacking rather than aggregations. This is possibly the key that CAF and NA, two solutes sharing many common structural features, undergo different clustering modes. The NA molecules were reported to form aggregate in aqueous solutions (Cui et al., 2010), while parallel stacking arises from CAF systems.

We further investigated the dynamic behaviors of the RBF + CAF + Water and CAF + Water systems by analyzing the mean square displacements (MSDs) of the centers of RBF and CAF molecules in the last 1 ns of the MD runs. The results are compared in Fig. 9. It is readily seen that the MSD–time curves of CAFs in the RBF + CAF + Water and CAF + Water systems are very close, confirming again that the parallel stacking occurred in these two systems are highly correlated. No plateau is observed for both curves, indicating that the clusters in both systems are still quite mobile. The MSD–time curve of RBF in the RBF + CAF + Water system, on the other hand, trends a relative lower slope in addition to significant plateauing. It was suspected initially that the plateauing may be attributed to the impediment in molecular movement of RBF imposed by the stacking with the CAFs. To confirm this, another system containing one RBF and 3000 water molecules (RBF + Water system) was constructed and subsequently subjected to a 3 ns MD run under the same conditions described above. The MDS-time curve of RBF in the last 1 ns was calculated and plotted in Fig. 9. It is seen that, despite that the curve trends initially a much higher slope than that of the RBF + CAF + Water system, which indicates that the stacking of solutes in the latter indeed hampers the mobility of

RBF, this curve plateaus after 300 ps as well. It thus seems that the plateauing is not due to the stacking of RBF with CAFs. Furthermore, since the RBF + Water system contains only one RBF molecule, it is impossible to observe a potential phase separation and solidification of RBF in this system. Therefore, the plateauing of MSD–time curves does not signify the solidification of RBF, despite that it indeed reflects the immobility of RBF in the RBF + Water system. We further examined the MSD–times curves of water molecules in the RBF + CAF + Water and the RBF + Water systems, and compared them with that in the pure Water system (data not shown). The three curves are almost overlapping, indicating that the mobility of water has not been affected by the immobility of RBF in the former two systems. This implicates that a gelation or thickening of the RBF solutions is unlikely to arise at this concentration. So far we have not found a reasonable explanation to account for the immobility of RBF showed above. Note that the MSD–time curves in Fig. 9 present certain variations, which are likely owing to the worsening statistics arising from the small numbers of solute molecules in our models. To check the reliability of the calculated results, we further calculated the MSD in the second to the last 1 ns of each run (data not shown), and compared them with those above. The results are quite consistent, showing that the results in Fig. 9 are reliable.

The diffusion coefficients (D) of CAF derived from slopes of the MSD–time curves via D = slope/6 are 0.362 and 0.424 (10^{-9} m^2/s) for the RBF + CAF + Water and CAF + Water systems, respectively, which fall in the typical range of diffusion coefficients in liquids (the bulk data of diffusion coefficients in liquids appear in the magnitude of 10^{-9}–10^{-10} m^2/s (Wilke and Chang, 1955; Hayduk and Laudie, 1974; Chen and Othmer, 1962)). The results not only confirm that the molecular stacks in the RBF + CAF + Water and CAF + Water systems are still in liquid state, but also demonstrate a strong correlation in dynamic movements of the aggregates in these systems. We then estimated the diffusion coefficient of CAF in a dilute aqueous solution by invoking the Wilke and Chang (1955) method as improved by Hayduk and Laudie (1974). The estimation gave a diffusion coefficient of 0.779×10^{-9} m^2/s, which is about 2-fold higher than the values above. This trend is consistent to our earlier report on NA solutions (Cui et al., 2010), where the cause has been identified as the impediment of molecular displacement entailed by the solute clustering. The estimation based upon the Wilke and Chang method assumes a dilute solution, where solute–solute interactions are not taken into consideration, whereas in our simulation studies the solute–solute interactions are prevalent and play a critical role in slowing the dynamics of the solutes. Hence, the above simulated results are considered reasonable. In the case of RBF, on the other hand, the calculation of diffusion coefficient was not pursued due to the plateauing of the MSD–time curves.

To summarize, this study finds significant structural evidences supporting the occurrence of parallel stacking of CAF and RBF molecules as well as of the self-stacking of CAF molecules in aqueous solutions. This finding conforms to other studies on these solutions employing NMR spectrometry (Evstigneev et al., 2005; Davies et al., 2001a) and suggests that the hydrotropic solubilization effect of CAF may arise from the molecular stacking of CAF and the hydrophobic solutes. The high correlation in both structure and dynamics between the CAF solution and the RBF + CAF solution, as demonstrated in RDFs, in changes in HB interactions and various energy components, and in the dynamic movements, suggests that the self-stacking of CAF is the primary phenomenon, while the incorporation of RBF into the stack is the secondary effect. Both effects, however, are likely to arise from the same mechanism, which is the restoration of normal water structure that was disrupted by the dispersion of these specific solutes. As the result of this restoration, the total system energy is minimized. Furthermore, in comparison to our earlier study on NA solutions (Cui et al., 2010), it is evident that the clustering mechanism of CAF and NA are different, with the former developing parallel stacking and the latter forming molecular aggregates. This finding defies the conclusions from some earlier studies on the NA system (Veselkov et al., 2002; Evstigneev et al., 2006). Since both NA and CAF are heteroaromatic molecules with flat configurations, it appears that the aromatic nature and flat molecular configuration alone are insufficient, albeit they may be necessary, in leading to the parallel stacking. Although further studies are required to elucidate what mechanism drives the different solute clustering modes, we speculate that the parallel stacking, relative to the molecular aggregation, may impose a stricter requirement on the solute molecular structures. This may explain that NA has been reported to solubilize a much wide range of compounds, and thereby a much more common solubilizer, than CAF. On the other hand, a flat aromatic ring structure may be a necessary precondition for the solutes to be incorporated in the parallel stacking. This offers an explanation for the observation that many compounds reported to be solubilized by CAF feature aromatic structures (Davies et al., 2001a,b).

One point worth noting is the molecular cluster size. In the RBF + CAF + Water system, the system appears stabilize with one CAF molecule not incorporated in the molecular stack, implicating that the cluster may have a maximum size in equilibrium with the free floating solute. This result was not observed in the NA solution reported before (Cui et al., 2010). One potential cause that may give rise to this difference could be the periodic boundary condition (PBC) adopted in our models. The current study employs a box containing 3000 water and 6–7 solutes, while in the cases of NA and urea derivatives the models consisted of 1000 water molecules and 38–73 solutes. The smaller box size and higher solute concentrations in the NA and urea derivatives systems likely gave rise to more prominent artifacts due to PBC, because solute molecules forced by the PBC to re-enter the box from the opposite side may interact artificially with other discrete aggregates and finally result in a single large aggregate. This effect moderated with larger box sizes and lower solute concentrations. As seen in the current study, the final molecular stack size (length) is approximately 14.8 Å, while the box length is >45 Å (the RBF + CAF + Water system). The odds for a solute molecule re-entering the box to induce a single larger cluster are much lower relative to the NA and urea derivatives systems. In the case of the RBF + CAF + Water system, for instance, even the last floating CAF molecule had once clustered with the stack (at 3.5 ns), it still managed to drift away after just a short period of time (<0.5 ns). It seems, therefore, that the simulation studies are likely to over-estimate the cluster size due to the PBC constraint, and the degree of the over-estimation is dependent on the model size and solute concentration.

Another finding that should be highlighted is the role of specific solute–solute interactions in the clustering. In the systems studied here no CAF–CAF HBs were found. Yet, solute parallel stacking was still developed in the CAF + Water system. This clearly shows that solute–solute interactions are not the determining factor, albeit they may be instrumental, to solute clustering.

Finally, we may comment on the role of aromaticity vs. hydrophobicity in hydrotropic solubilization. In the CAF solution in this study and the NA system reported previously (Cui et al., 2010), the primary driving force for the solubilization effect is the same, which is the restoration of normal water structure through solute clustering, despite that the modes of clustering may be different. It appears that the aromaticity and the hydrophobicity have accomplished the same outcome via similar, if not exact the same, mechanism. We have not found an apparent quantitative difference in the effectiveness of these two classes of structures. Based upon what we observed so far, the balance between the hydrophobicity and hydrophilicity of the hydrotropic agents may be more important. The former enhances the solute clustering, while the latter keeps the clusters in the aqueous phase avoiding

phase separation. This is consistent to the observations of some authors (Lee et al., 2003). This effect may be obscured by the diverse structures of hydrotropic agents, and led to the debate over the role of the aromaticity and the hydrophobicity.

References

Agrawal, S., Pancholi, S.S., Jain, N.K., Agrawal, G.P., 2004. Hydrotropic solubilization of nimesulide for parenteral administration. Int. J. Pharm. 274, 149–155.

Birdsall, B., Feeney, J., Partington, P., 1973. Ionization, self association, and proton exchange studies of nicotinamide in aqueous solution using NMR spectrometry. J Chem. Soc. Perkin Trans. 2, 2145–2151.

Boylan, J., 1986. Liquids. In: Lachman, L., Lieberman, H.A., Kanig, J.L. (Eds.), The Theory and Practice of Industrial Pharmacy, 3rd ed. Lea and Febiger, Philadelphia, PA, p. p. 246.

Bunte, S.W., Sun, H., 2000. Molecular modeling of energetic materials: the parameterization and validation of nitrate esters in the COMPASS force field. J. Phys. Chem. B 104, 2477.

Cheema, M.A., Siddiq, M., Barbosa, S., Castro, E., Egea, J.A., Antelo, L.T., Taboada, P., Mosquera, V., 2007. Compressibility, isothermal titration calorimetry and dynamic light scattering analysis of the aggregation of the amphiphilic phenothiazine drug thioridazine hydrochloride in water/ethanol mixed solvent. Chem. Phys. 336, 157–164.

Chen, N.H., Othmer, D.F., 1962. New generalized equation for gas diffusion coefficient. J. Chem. Eng. Data 7, 37–41.

Coffman, R.E., Kildsig, D.O., 1996a. Hydrotropic solubilization-mechanistic studies. Pharm. Res. 13, 1460–1463.

Coffman, R.E., Kildsig, D.O., 1996b. Effect of nicotinamide and urea on the solubility of riboflavin in various solvents. J. Pharm. Sci. 85, 951–954.

Cui, Y., Xing, C., Ran, Y., 2010. Molecular dynamics simulations of hydrotropic solubilization and self-aggregation of nicotinamide. J. Pharm. Sci. 99 (7), 3048–3059.

Davies, D.B., Veselkov, D.A., Evstigneev, M.P., Veselkov, A.N., 2001a. Self-association of the antitumor agent novatrone and its hetero-association with caffeine. J. Chem. Soc. Perkin Trans. 2, 61–67.

Davies, D.B., Veselkov, D.A., Djimant, L.N., Veselkov, A.N., 2001b. Hetero-association of caffeine and aromatic drugs and their competitive binding with a DNA oligomer. Eur. Biophys. J. 30, 354–366.

Evstigneev, M.P., Evdtigneev, V.P., Santiago, A.A., Davies, D.B., 2006. Effect of a mixture of caffeine and nicotinamide on the solubility of vitamin B2 in aqueous solution. Eur. J. Pharm. Sci. 28, 59–66.

Evstigneev, M.P., Rozvadovskaya, A.O., Santiago, A.A., Mukhina, Y.V., Veselkov, K.A., Rogova, O.V., Davies, D.B., Veselkov, A.N., 2005. A ^{1}H NMR study of the association of caffeine with flavine mononucleotide in aqueous solutions. Russ. J. Phys. Chem. 79, 573–578.

Falk, M., Gil, M., Iza, N., 1990. Self-association of caffeine in aqueous solution: an FT-IR study. Can. J. Chem. 68, 1293–1299.

Fawzi, M., Davison, E., Tute, M., 1980. Rationalization of drug complexation in aqueous solution by use of Hückel frontier molecular orbitals. J. Pharm. Sci. 69, 104–106.

Guttman, D.E., Athalye, M.Y., 1960. Solubilization of riboflavin by complex formation with caffeine, theophylline, and dimethyluracil. J. Am. Pharm. Assoc. 49, 687–691.

Hata, S., Mizuno, K., Tomioka, S., 1967. Effects of electron donors on photodecomposition of menadione in aqueous solution 1. Interaction between electron donors and menadione in aqueous solution. Chem. Pharm. Bull. 15, 1719–1795.

Hayduk, W., Laudie, H., 1974. Pediction of diffusion coefficients for nonelectrolytes in dilute aqueous solutions. AIChE J. 20, 611–615.

Hwang, M.J., Stockfisch, T.P., Hagler, A.T., 1994. Derivation of Class II force-fields. 2. Derivation and characterization of a Class-II force-field, CFF93, for the alkyl functional-group and alkane molecules. J. Am. Chem. Soc. 116, 2515.

Kenley, R.A., Jackson, S.E., Winderle, J.S., Shunko, Y., Visor, G.C., 1986. Water soluble complexes of the antiviral drugs, 9-[(1,3-dihydroxy-2-propoxy)methyl]guanine and acyclovir: the role of hydrophobicity in complex formation. J. Pharm. Sci. 75, 648–653.

Lee, J., Lee, S.C., Acharya, G., Chang, C., Park, K., 2003. Hydrotropic solubilization of paclitaxel: analysis of chemical structures for hydrotropic property. Pharm. Res. 20, 1022–1030.

Neuberg, C., 1916. Hydro-tropical appearance I Announcement. Biochem. Z. 76, 107–176.

Oberoi, L.M., Alexander, K.S., Riga, A.T., 2005. Study of interaction between ibuprofen and nicotinamide using differential scanning calorimetry, spectroscopy, and microscopy and formulation of a fast-acting and possibly better ibuprofen suspension for osteoarthritis patients. J. Pharm. Sci. 94, 93–101.

Rasool, A.A., Hussain, A.A., Dittert, D.W., 1991. Solubility enhancement of some water-insoluble drugs by nicotinamide and related compounds. J. Pharm. Sci. 80, 387–393.

Shah, S.P., Flanagan, D.R., 1990. Solubilization of salicylamide and acetaminophen by antihistamines in aqueous solution. J. Pharm. Sci. 79, 889–892.

Sun, H., 1998. COMPASS: an ab initio force-field optimized for condensed-phase: applications overview with details on alkane and benzene compounds. J. Phys. Chem. B 102, 7338.

Suzuki, H., Sunada, H., 1980. Mechanistic studies on hydrotropic solubilization of nifedipine in nicotinamide solution. Chem. Pharm. Bull. 46, 125–130.

Veselkov, A.N., Lantushenko, A.O., Chubarov, A.S., Veselkov, D.A., Davies, D.B., 2002. ^{1}H NMR analysis of the self-association of riboflavine-mononucleotide and its complexation with nicotinamide in an aqueous solution. Russ. J. Phys. Chem. 76, 1350–1356.

Wilke, C.R., Chang, P., 1955. Correlation of diffusion coefficients in dilute solutions. AIChE J. 1, 264–270.